Virology 385 (2009) 444–454

Contents lists available at ScienceDirect

Virology

journal homepage: www.elsevier.com/locate/yviro

Betanodavirus non-structural protein B1: A novel anti-necrotic death factor that modulates cell death in early replication cycle in fish cells

Lei-Jia Chen [1], Yu-Chin Su [1], Jiann-Ruey Hong *

Laboratory of Molecular Virology and Biotechnology, Institute of Biotechnology; National Cheng Kung University, Tainan 701, Taiwan

ARTICLE INFO

Article history:
Received 7 October 2008
Returned to author for revision
3 November 2008
Accepted 25 November 2008
Available online 10 January 2009

Keywords:
Betanodavirus
B1 protein
Gain-of-function
Anti-sense RNA
Mitochondria
Anti-necrotic gene

ABSTRACT

The functions of the Betanodavirus non-structural protein B1 is still unknown. We examined B1 expression patterns and investigated novel cell death regulatory functions for this viral protein following RGNNV infection in fish cells. The *B1* gene (336 nt) was cloned from the redspotted grouper nervous necrosis virus (RGNNV) genome. *B1* mRNA was rapidly expressed in the fish cells from viral RNA3 at 12 h post-infection (p.i.). At the protein level, expression was low at 12 h p.i., and then increased rapidly between 24 h and 72 h p.i. In RGNNV-infected, B1-containing fish cells, over expression of RGNNV B1 reduced Annexin-V positive cells by 50% and 65% at 48 h and 72 h p.i., respectively, and decreased loss of mitochondrial membrane potential (MMP) by 20% and 70% at 48 h and 72 h p.i., respectively. Finally, B1 knockdown during RGNNV infection using anti-sense RNA increased necrotic cell death and reduced cell viability during the early replication cycle (24 h p.i.). Our results suggest that B1 is an early expression protein that has an anti-necrotic cell death function which reduces the MMP loss and enhances viral host cell viability. This finding provides new insights into RNA viral pathogenesis and disease control.

Introduction

Betanodaviruses cause viral nervous necrosis (VNN), an infectious neuropathological condition in fish that is characterized by necrosis of the central nervous system, including the brain and retina. VNN necrosis is accompanied by clinical signs such as abnormal swimming behavior and development of a darker body color (Bovo et al., 1999). This disease is capable of causing mass mortality in the larval and juvenile populations of several teleost species and is of global economic importance (Munday et al., 2002). Despite their potentially severe impact on the aquaculture industry, betanodaviruses have not been well studied. Characterization of betanodavirus molecular regulation processes would aid in deciphering the mechanism(s) of viral pathogenesis and infection.

The family *Nodaviridae* is comprised of the genera *Alphanovirus* and *Betanovirus*. *Alphanovirus* predominantly infects insects, while *Betanovirus* predominantly infects fish (Ball and Johnson, 1999; Schneemann et al., 1998; Toffolo et al., 2006). Nodaviruses are small, non-enveloped, spherical viruses with bipartite positive-sense RNA genomes that are capped but not polyadenylated (Toffolo et al., 2006). The largest genomic segment, RNA1, is a component of the viral RNA-dependent RNA polymerase (RdRp) that encodes protein A (Nagai and Nishizawa, 1999). The middle genomic segment, RNA2, encodes a capsid protein (Nishizawa et al., 1995) which may also function in the induction of cell death (Guo et al., 2003). Alphanoviruses also synthesize RNA3, a sub-genomic RNA species from the 3′ terminus of RNA1. RNA3 contains two putative open reading frames that potentially encode an 111 amino acid protein (B1) and a 75 amino acid protein (B2) (Ball and Johnson, 1999; Schneemann et al., 1998; Johnson et al., 2000). The B1-encoding region is in the same reading frame as the protein A coding region, which can be detected by cDNA clone transfection in Nodamura virus (NoV)-infected insect and animal cells (Johnson et al., 2003). The functional role of B1 is still unknown. On the other hand, the B2-encoding region is present in the +1 reading frame with respect to protein A, and overlaps with the entire C terminal region of protein A. B2 is a potent suppressor of host siRNA silencing in alphanodaviruses, including nodavirus flock house virus (FHV), and NoV in *Drosophila* (Wang et al., 2006), animals (Li et al., 2002), and *Caenorhabditis elegans* (Lu et al., 2005); and in betanodaviruses such as striped jack nervous necrosis virus in fish (Iwamoto et al., 2005), which may function as an inducer of host necrotic cell death (Chen et al., 2007; Su et al., 2009).

Apoptosis is a genetically controlled event with defined roles in tissue development, homeostasis, and disease (Kerr and Harmon, 1991; Majno and Joris, 1995; Wyllie et al., 1980). Apoptosis and necrosis are the two prototypical mechanisms by which nucleated eukaryotic cells die (Kerr and Harmon, 1991; Majno and Joris, 1995; Wyllie et al., 1980). Necrosis is considered to be a pathological reaction that occurs in response to major perturbations in the cellular environment such as a lytic viral infection, while apoptosis represents a physiological process that is part of homeostatic tissue regulation during normal turnover (Kerr and Harmon, 1991). Necrosis is

* Corresponding author. Fax: +886 6 2766505.
E-mail address: jrhong@mail.ncku.edu.tw (J.-R. Hong).
[1] These authors contributed equally to the research.

0042-6822/$ – see front matter © 2008 Elsevier Inc. All rights reserved.
doi:10.1016/j.virol.2008.11.048

characterized by severe pathophysiological changes, including mitochondrial swelling, plasma membrane disruption and ultimately leakage of cellular contents into the interstitial space. This latter event triggers acute exudative inflammation of the surrounding tissue, with the subsequent activation and infiltration of neutrophils into the area thought to increase intracellular digestive enzyme activation (Gukovskaya et al., 2002; Criddle et al., 2007). In addition, cell necrosis can also be regulated and may in some cases involve activation of proteolytic caspases (Schwab et al., 2002).

In previous studies, we have demonstrated that the redspotted grouper nervous necrosis virus (RGNNV) TN1 strain can induce apoptosis before necrosis in a grouper liver cell line (GL-av). Then, we found that RGNNV infection can induce loss of the mitochondrial membrane potential (MMP) in GL-av cells, which MMP loss also blocked by either mitochondrial membrane permeability (MMP) transition pore inhibitor BKA (Chen et al., 2006a) or the Bcl-2 family member protein zfBcl-x_L (Chen et al., 2006b, 2007). On the other hand, in viral genome encoding first one viral death inducer protein α (42 kDa) was reported by Dr. Guo et al. (2003), which can activate caspase-3 for triggering apoptotic cell death. Furthermore, protein α can induce post-apoptotic necrosis through a mitochondrial-mediated mechanism in grouper fin (GF-1 cell) cell line (Wu et al., 2008), which protein α-induced MMP loss could be blocked by over expression of the Bcl-2 family member zfBcl-x_L (Wu et al., 2008). Recently, the

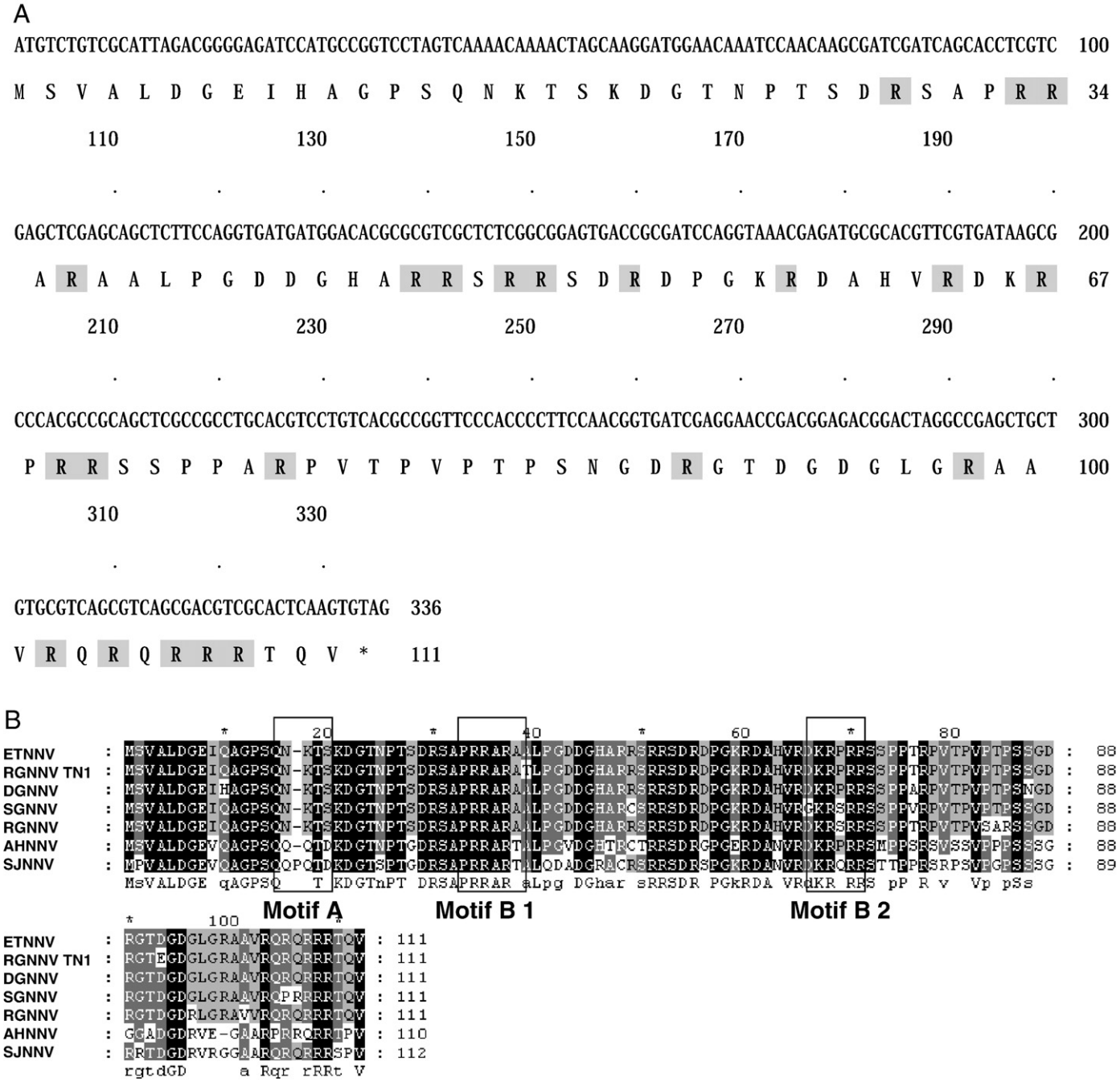

Fig. 1. Alignment of deduced amino acid sequences of RGNNV TN1 B1. (A) The primary structure of B1 in the RGNNV TN1 strain. The arginine-rich residues are shown in shaded blocks. (B) Alignment of the deduced amino acid sequence of RGNNV TN1 B1 with the corresponding sequences of other betanodavirus proteins. The conserved amino acids for residues common to at least seven betanodavirus proteins are shown in black blocks and the potential N-glycosylation site is indicated by motif A, which corresponds to residues 16–19 (NKTS). Potential nuclear localization signals are indicated by motif B1, corresponding to residues 33–38 (PRRARA), and motif B2, corresponding to residues 67–771 (KRPRR).

second one viral genomic encoding death factor B2, can induce fish cell death via bax-mediated pathway (Su et al., 2009). In the present study, we demonstrate that the non-structural *B1* gene is an early expression gene that contributes to an anti-necrotic death function in early replication stage and which may regulate the cell death via reduce MMP loss. Our observations further the current understanding of betanodavirus pathogenesis and may contribute to the future development of methods for disease control.

Results

Cloning of RGNNV B1 and determination of functional domains

B1 cloned using specific primers derived from different RGNNV TN1 sequences was used to synthesize a 336 bp sequence from the genome of viral particles isolated from RGNNV TN1-infected GF-1 cells. The sequences of positive clones from the ligation reaction were used to search GenBank databases. Significant matches were made after the nucleotide sequences were translating into amino acid residues (Fig. 1A). These matches displayed an arginine-rich region between amino acids 29–108 (shown in shaded blocks) and comprised 19.8% of the total amino acids. The arginine-rich residues likely have important functions such as forming an arginine-rich nuclear localization sequence (Michaud et al., 2008) or forming an arginine-rich groove for RNA binding to nucleoproteins (Ng et al., 2008).

When the nucleotide sequence identity of the RGNNV TN1 strain (EU118118) (Figs. 1A, B) was compared with other species, there was a 96% match with epinephelus tauvina nervous necrosis virus (ETNNV; AF3195555), 95% with dragon grouper nervous necrosis virus (DGNNV; AY721616), 94% with greasy grouper nervous necrosis virus (GGNNV; AY369136), 92% with sevenband grouper nervous necrosis virus (SGNNV; AY324869), 81% with Atlantic halibut nervous necrosis virus (AHNNV; AJ401165), and 70% with striped jack nervous necrosis virus (SJNNV; AB025018).

Based on sequence analyses, the predicted molecular weight for B1 was 12.1 kDa and the theoretical pI value was 11.76 (Fig. 1B). The potential N-glycosylation site is indicated by motif A, corresponding to residues 16–19 (Box A; NKTS; PROSITE). The potential discrimination of nuclear localization signals is indicated by motif B1 (Fig. 1B; PROSITE) corresponding to residues 33–38 (PRRARA), and motif B2 corresponding to residues 67–71 (KRPRR) (Falquet et al., 2002).

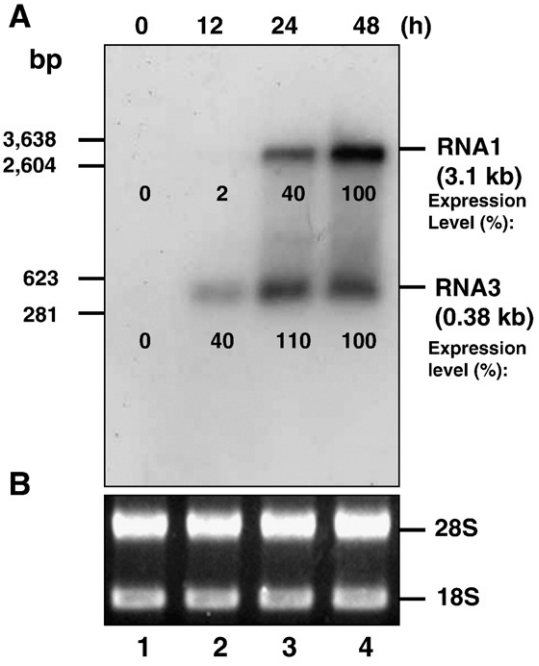

Fig. 2. Northern blot identification of RGNNV *B1* gene probed and cross-reacted with genomic RNA1 and sub-genomic RNA3. (A) Lanes 2–5 represent RGNNV-infected GF-1 cells incubated for 0, 12, 24, and 48 h that were probed with *B1* cDNA for tracing of RNA1 and RNA3 genomes. (B) 18S and 28S served as internal controls.

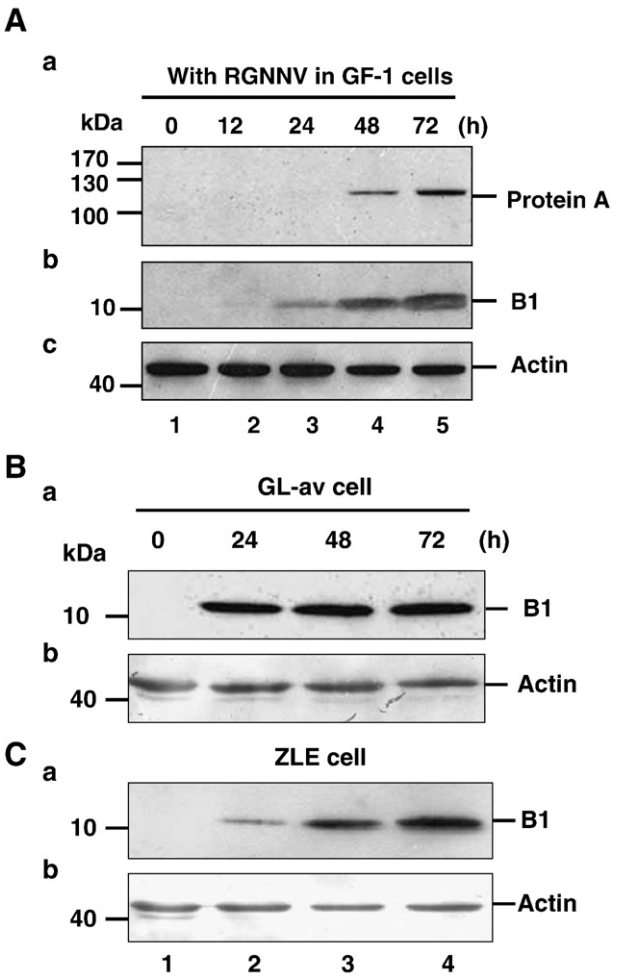

Fig. 3. Western blot identification of the RGNNV B1 expression pattern in fish cell lines. (A:a–b) B1 protein expression in GF-1 cells is shown at 0 h (lane 1), 12 h (lane 2), 24 h (lane 3), 48 h (lane 4), and 72 h (lane 5) following infection with RGNNV TN1 (m.o.i.=1). Protein A (A:a) and RGNNV TN1 B1 (A:b) expression were detected in gels using Western immunoblotting with RGNNV B1 polyclonal antibody. (A:c) Actin expression served as an internal control. (B and C) B1 protein expression in GL-av (B:a) and ZLE (C:a) cells at 0 h (lane 1), 24 h (lane 2), 48 h (lane 3), and 72 h (lane 4) after infection with RGNNV (m.o.i.=1). Protein B1 expression in GL-av cells (B:a) and in ZLE cells (C:a) was detected by Western immunoblotting with a RGNNV B1 polyclonal antibody. (B:b and C:b) The internal control protein actin for B:a and C:a, respectively.

Identification of B1 is as an early expression gene in grouper fish cells

Using a grouper fish cell system, we determined whether *B1* was expressed in the viral genome during infection. *B1* cDNA was used as a probe for detection of *B1 in RNA1 or its derivative sub-genomic RNA3. B1* was rapidly detected in RNA3 at approximately a 40% expression level 12 h after initiation of infection (Fig. 2A, lane 3), and at expression levels of 110% and 100% after 24 and 48 h, respectively (Fig. 2A, lanes 4 and 5, respectively). *B1* expression was detected in RNA1 later than in RNA3. In RNA1, *B1* expression levels in GF-1-infected cells were 2% at 12 h (Fig. 2A, lane 3), 40% at 24 h (Fig. 2A, lane 4), and 100% at 48 h (Fig. 2A, lane 5). The internal control 18S and 28S are shown in Fig. 2B.

Identification of B1 protein expression pattern in different fish cell lines

Whether the RGNNV protein B1 was expressed in fish cell remained to be determined, since alphanovirus B1 protein was barely detectable in cDNA clone-transfected host cells (Johnson et al., 2003). To answer this question, a RGNNV B1 polyclonal antibody was produced and used to detect B1 protein expression. Results indicate that B1 production occurs rapidly after infection, with a few of expressions evident at 12 h, then larger amount expression at 24 h after establishment of infection (Fig. 3A:b, lane 2). The electrophoretically-determined molecular weight of the protein was 12.1 kDa (Fig. 3A:b, lanes 2–5). Complementing the consistent

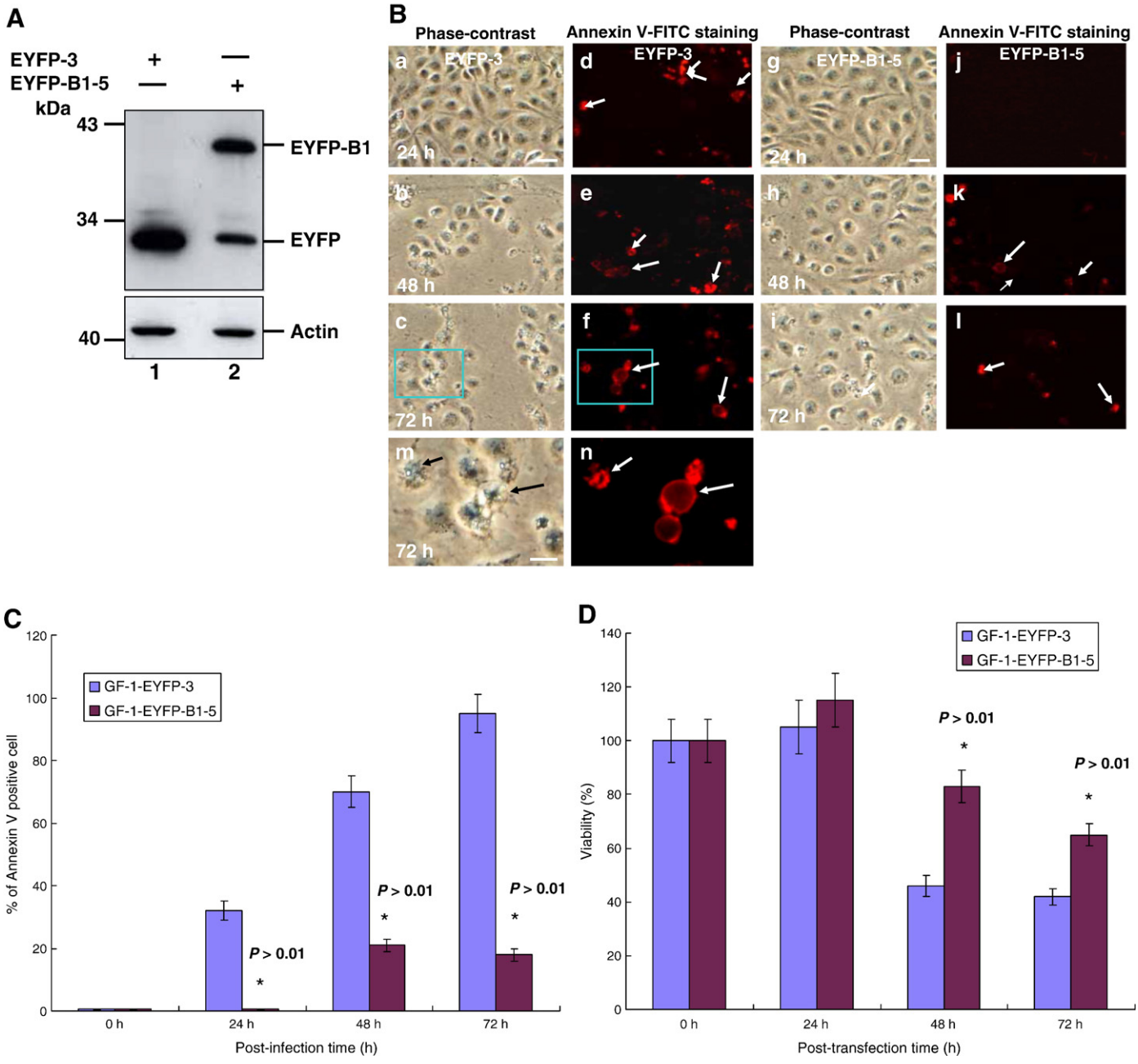

Fig. 4. Influence of B1 over expression on GF-1 cell viability during RGNNV infection. GF-1 cells transfected with EYFP-C1 or EYFP-B1 plasmid were incubated and selected with G418. Single colonies were selected for the experiments. (A) Western blot analysis of EYFP-B1 and EYFP protein expression with against RGNNV B1 polyclonal antibody in stably expressing cell lines. Lane 1, clone EYFP-3; lane 2, clone EYFP-B1–5. Actin served as an internal control. (B) Phase-contrast and fluorescence images showing the morphology of post-apoptotic, necrotic RGNNV-infected GF-1-EYFP-3 and GF-1-EYFP-B1–5 cells (m.o.i.=1) at 24, 48, and 72 h post-transfection. Post-apoptotic, necrotic cells are present (B, e, f and n; indicated by long arrows). Phase-contrast (EYFP-3: B, a–c and m; EYFP-B1–5: B, g–i) and fluorescence image (EYFP-3: B, d–f; EYFP-B1–5: B, i–l) showing the morphology of annexin V-labeled post-apoptotic necrotic cells expressing either EYFP-3 (B: d–f and n; indicated by long arrows) or EYFP-B1–5 (B: i, k, and l). (C) The percentage of apoptotic and post-apoptotic, necrotic cells producing EYFP or EYFP-B1 at 0, 24, 48, and 72 h after transfection with RGNNV TN1 (m.o.i.=1). The percentages of apoptotic and post-apoptotic, necrotic EYFP- and EYFP-B1-producing cells. Data are the percentage of 200 cells and were determined at each time point in triplicate; with each point representing the mean of 3 independent experiments. Error bars represent SEM. Data were analyzed using either paired or unpaired Student's *t*-tests as appropriate. $p<0.05$ was taken to represent a statistically significant difference between mean values of groups. (D) The viability of EGFP- and EYFP-B1-producing GF-1 cells infected with GRNNV was determined at 0, 24, 48, and 72 h post-transfection in triplicate. Each point represents the mean viability from three independent experiments. Error bars represent SEM. Data were analyzed using either paired or unpaired Student's *t*-tests as appropriate. $p<0.05$ was taken to represent a statistically significant difference between mean values of groups.

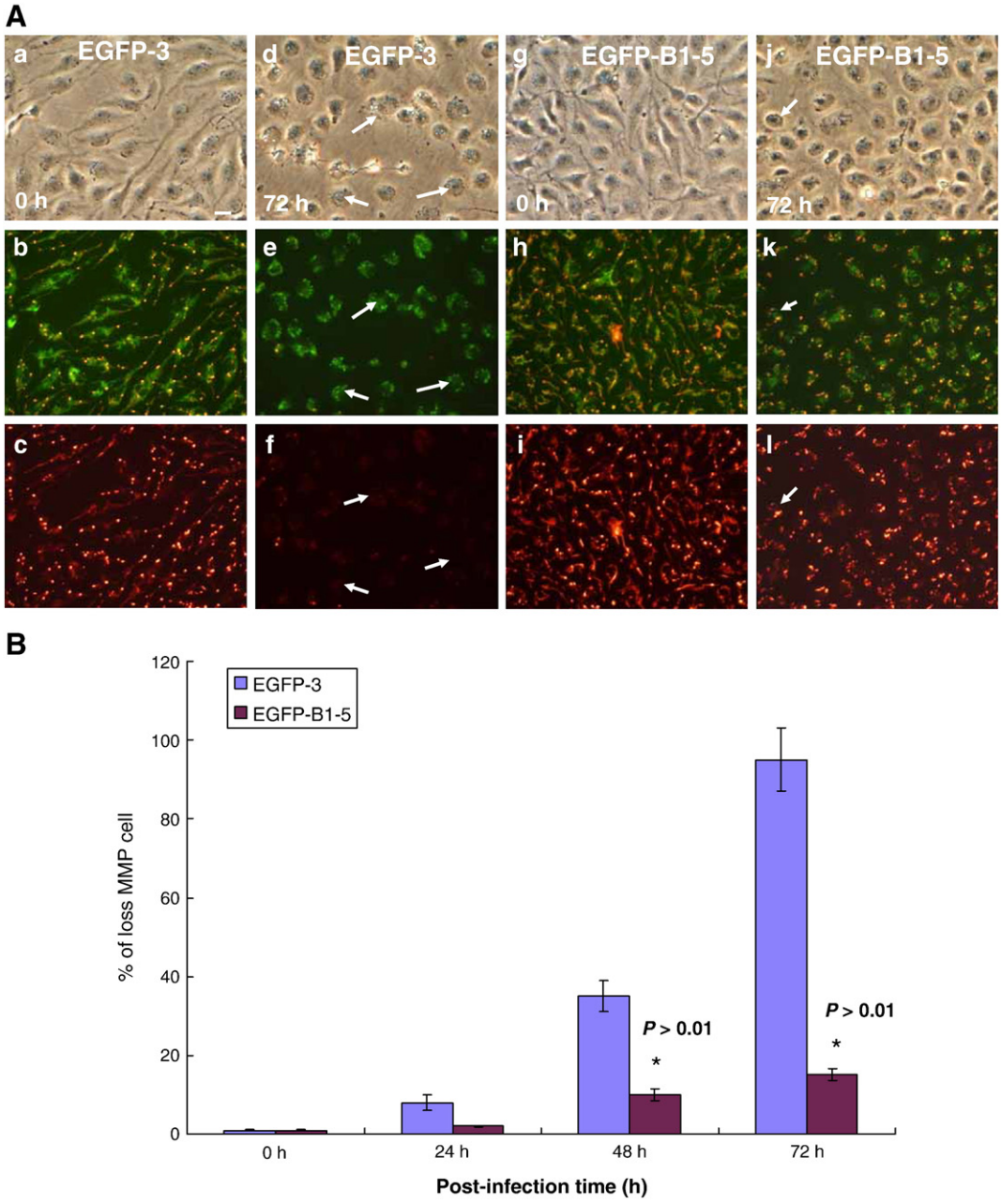

Fig. 5. B1 protein over expression can effectively block MMP loss following RGNNV infection in GF-1-B1 stably expressing cells. Investigation of whether B1 protein can reduce RGNNV-induced MMP loss in GF-1-EGFP-B1–5 and GF-1-EGFP-3 cells at 0 and 72 h p.t. Normal control cells (Panel A: a–c), EGFP-3-contained cells (Fig. 4A: d–f), and EGFP-B1–5-contained cells at 0 h (Fig. 4A: g–i). RGNNV-infected cells with a loss of MMP at 72 h p.i are indicated by arrows (EGFP-3 cells at d–f; EGFP-B1–5 cells at j–l). Scale bar = 10 μm. (B) Identification of B1 prevents MMP loss in GF-1-EGFP-B1–5 and GF-1-EGFP-3 cells at 0, 24, 48, and 72 h. The number of positive cells per 200 cells in each sample was counted in three individual experiments. Data were analyzed using either paired or unpaired Student's *t*-tests as appropriate. $p<0.05$ was taken to represent a statistically significant difference between mean values of groups.

Northern blot results shown in Fig. 2A, lanes 1–4, showing *B1* as an early expression gene, B1 protein expression increased thereafter, as was evident 24, 48, and 72 h after infection (Fig. 3A:b, lanes 3–5, respectively). On the other hand, we also found that the B1 polyclonal antibody recognized the protein A protein between 48 h and 72 h p.i. (Fig. 3A:a, lanes 4–5), which was subgenomically

Fig. 6. Effect of RGNNV B1 knockdown by its anti-sense RNA on GF-1 cell viability during RGNNV infection. GF-1 cells transfected with pCDNA3.1 and pCDNA3.1-B1 anti-sense RNA plasmid were incubated and selected with G418. Single colonies were selected for the experiments. (A) Western blot analysis of EYFP-B1 and EYFP protein expression. The stable cell lines pCDNA3.1, pCDNA3.1-B1 anti-sense RNA-4 and -9 transfected with pEYFP-B1 (1 μg/per 6 cm^2 dish) were used to test knockdown effects 24 h p.t. Lanes 1–3, Vector-based (pCDNA3.1) stably-expressing cell line (pCDNA3.1-2); lanes 4–6, pCDNA-B1 anti-sense-4 stably-expressing cell line; and lanes 7–9, pCDNA-B1 anti-sense-9 stably-expressing cell line. (B) Phase-contrast and fluorescence images showing the morphology of post-apoptotic, necrotic RGNNV-infected GF-1-pCDNA3.1-2 and GF-1-pCDNA3.1-B1 antisense RNA-9 cells (m.o.i. = 1) at 0, 24, 48, and 72 h post-transfection. Post-apoptotic, necrotic cells are present (B, e, f and n; indicated by long arrows). Phase-contrast (pCDNA3.1-2: B, a–d and m; B1 anti-sense RNA-9: B, i–l) and fluorescence images (pCDNA3.1-2: B, e–h; B1 anti-sense RNA-9: B, m–p) showing the morphology of annexin V-labeled post-apoptotic necrotic cells either pCDNA3.1-2 (B: f–h; indicated by arrows), or B1 anti-sense RNA-9 cells (B: n–p). (C) The percentage of apoptotic and post-apoptotic necrotic cells producing pCDNA3.1-2, B1 anti-sense RNA-9 at 0, 24, 48, and 72 h post-transfection. The percentages of apoptotic and post-apoptotic necrotic pCDNA3.1-2- and B1 anti-sense RNA-9-producing cells were determined in triplicate at each time point, with each point representing the mean of three independent experiments. Error bars represent SEM. Data were analyzed using either paired or unpaired Student's *t*-tests as appropriate. $p<0.05$ was taken to represent a statistically significant difference between mean values of groups.

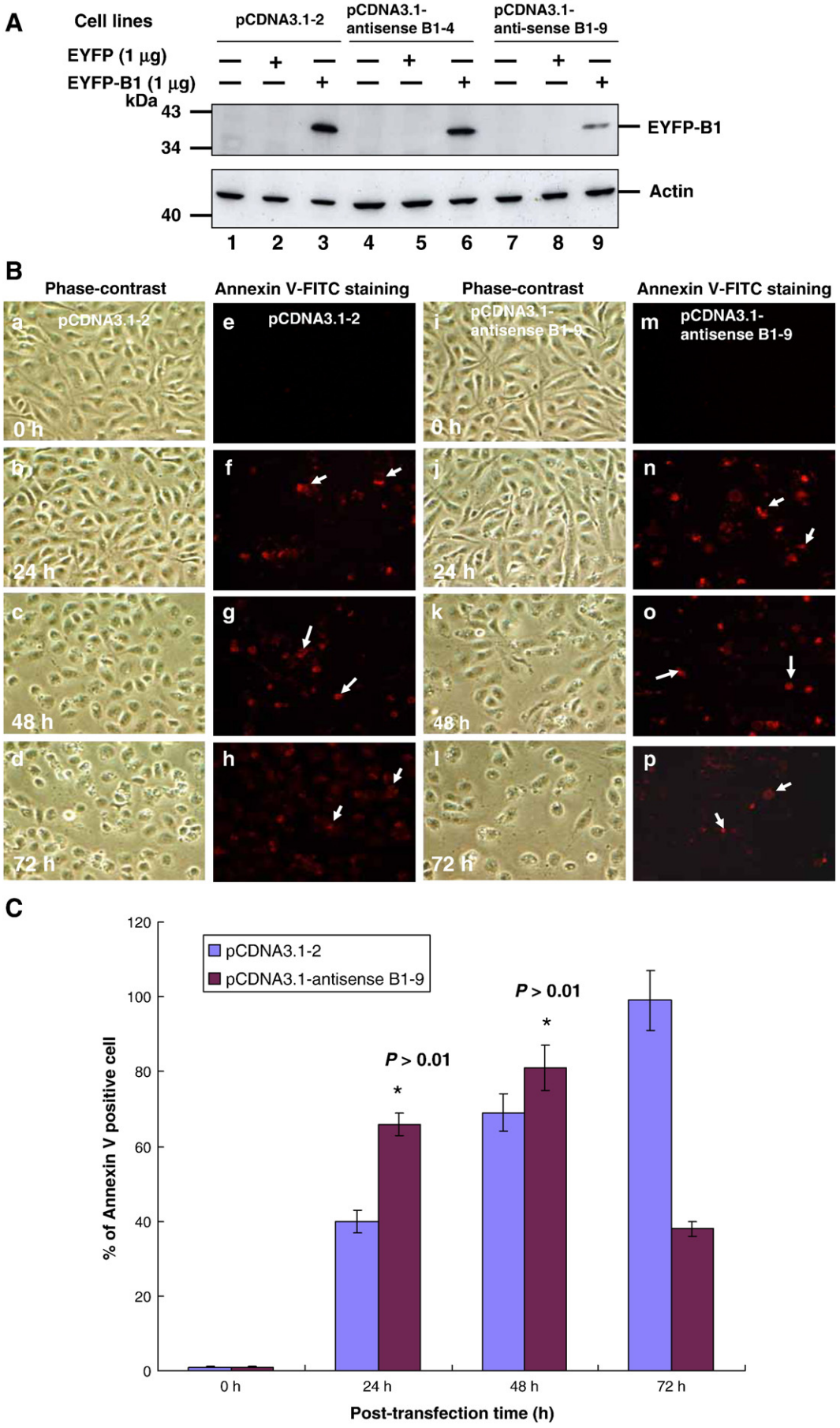
A
Cell lines
pCDNA3.1-2
pCDNA3.1-antisense B1-4
pCDNA3.1-anti-sense B1-9
EYFP (1 μg)
EYFP-B1 (1 μg)
kDa
43
34
40
EYFP-B1
Actin
1 2 3 4 5 6 7 8 9
B
Phase-contrast
Annexin V-FITC staining
Phase-contrast
Annexin V-FITC staining
a pCDNA3.1-2
e pCDNA3.1-2
i pCDNA3.1-antisense B1-9
m pCDNA3.1-antisense B1-9
0 h
24 h
48 h
72 h
C
pCDNA3.1-2
pCDNA3.1-antisense B1-9
P > 0.01
P > 0.01
% of Annexin V positive cell
0
20
40
60
80
100
120
0 h
24 h
48 h
72 h
Post-transfection time (h)

(336 bp) derived from the RNA1 (3.1 Kb) 3′-terminus in frame with RNA3. Expression of the internal control actin is shown in Fig. 3A:c, which have minus down-regulated after 48 h p.i. compared with 0 h. Furthermore, B1 protein was well expressed in two additional cell lines, GL-av (Fig. 3B:a, lanes 2–4) and ZLE (Fig. 3C:a, lanes 2–4), at 24 h and 48 h to 72 h p.i., respectively, demonstrating consistent results in fish cell expression systems. The internal control actin is shown in Figs. 3B, C:b.

Influence of B1 over expression on GF-1 cell necrosis and viability

EYFP- and EYFP-B1-expressing stable cell lines were generated in order to further investigate B1 functions. Western blotting confirmed the overproduction of the 44.1 kDa EYFP-B1 protein in GF-1 cells (the number 5 EYFP-B1-expressing stable cell line was designated as EYFP-B1–5; Fig. 4A, lane 2) and EYFP protein in GF-1 cells (the number 3 EYFP-expressing stable cell line was designated as EYFP-3; Fig. 4A, lane 1). In the functional assays, Annexin V-FITC staining showed reduced necrosis in B1-overproducing cells (Fig. 4B, panels g–i display phase-contrast micrographs, and panels j–l display red fluorescent micrographs) as compared with the EYFP control (Fig. 4A, panels a–c display phase-contrast micrographs and panels d–f display red fluorescent micrographs). Enlarged images (Fig. 4B; panels m and n are enlargements of panels c and f, respectively) clearly showed necrotic morphological changes (Fig. 4B, m, necrosis indicated by arrows) and necrotic cells with surface blebs (Fig. 4B, f, indicated by arrows) under phase-contrast microscopy. These morphological features indicated the translocation of phosphatidylserine from the inner leaflet to the outer leaflet of the plasma membrane in apoptotic and necrotic cells (Chen et al., 2006a, 2007).

Furthermore, as shown in Fig. 4C, more necrotic cells (0.5%, 32%, 70% and 95%) were induced by RGNNV infection in EYFP-3-expressing GF-1 cells than in EYFP-B1–5-expressing GF-1 cells (0.5%, 0.5%, 20%, and 18%) at 0, 24, 48, and 72 h p.i., respectively. Moreover, as shown in Fig. 4D, the viability of RGNNV-infected, EYFP-3-expressing GF-1 cells (100%, 104%, 45%, and 40% at 0, 24, 48, and 72 h p.i., respectively) was lower than RGNNV-infected, EYFP-B1–5-expressing GF-1 cells (100%, 115%, 82% and 65% at the same respective times). In particular, at 48 and 72 h p.i., EYFP-B1-expressing cells displayed enhanced cell viability (40% and 20%, respectively) when compared with EYFP-containing cells.

Over expression of B1 inhibits loss of MMP in GF-1 cells with RGNNV infection

To determine whether B1 over expression could block the loss of MMP in this RGNNV-induced necrotic cell death, mitochondrial function was evaluated using the MitoCapture Reagent (Apoptosis Detection, Mitochondria BioAssay™ Kit). The Mitocapture dye aggregates in the mitochondria of healthy cells and fluoresces red. In apoptotic or secondary necrosis cells, the dye cannot accumulate in mitochondria and fluoresces as green monomers in the cytoplasm. Results indicate that loss of MMP was more effectively blocked in infected GF-1 cells stably expressing B1 (EGFP-B1–5, 15% loss reduced to 2% at 24 h p.i., 35% loss reduced to 10% at 48 h p.i., and 95% loss reduced to 15% at 72 h p.i. (Fig. 5B); Fig. 5A: j–l; indicated by arrows) than in infected cells expressing EGFP (EGFP-3, Fig. 5A:d–f; indicated by arrows). Non-infected cells served as normal controls and are shown in Fig. 5A: g–i for EGFP-B1–5 containing cells, and in Fig. 5A: a–c for EGFP-3 containing cells.

Influence of B1 knockdown on GF-1 cell necrosis and viability

Moreover, to verify B1 cellular functions, we used a loss-of-function approach to determine whether the loss of B1 expression might enhance cell necrosis and reduce cell viability. Vector-containing (pCDNA3.1; as a negative control) and RGNNV antisense B1-containing stable cell lines (Weiss et al., 1999) were generated for further testing. Western blotting using the anti-B1 polyclonal antibodies confirmed the effective knockdown of *B1 in stable cell lines (pCDNA3.1, pCDNA3.1-antisense B1–4 and pCDNA3.1-antisense B1–9) transfected with the EYFP-B1 plasmid (1* μg/per plate in 6 cm per dish) for 24 h. The number 9 antisense B1 cell line showed better effective on knockdown of the 44.1 kDa EYFP-B1 protein in GF-1 cells (Fig. 6A, lane 9) than the number 4 antisense B1 cell line (Fig. 6A, lane 6) or the vector negative control (Fig. 6A, lane 3). The number 9 antisense B1 cell line was used for further functional assays.

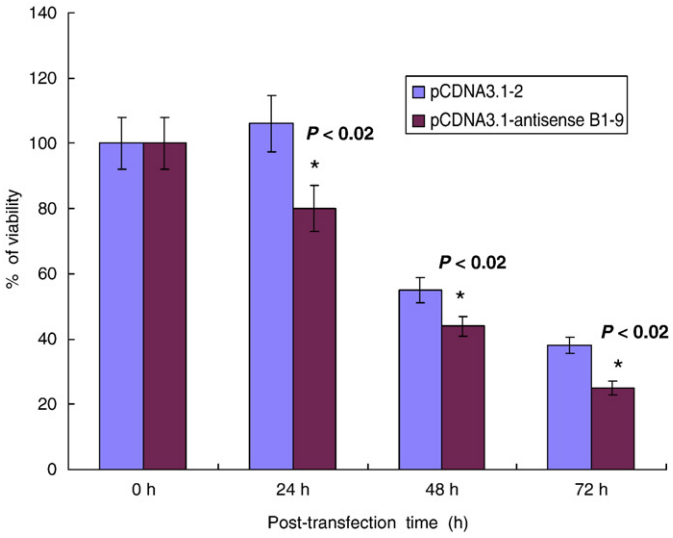

Fig. 7. Effects of B1 protein knockdown by its antisense RNA with RGNNV infection on host cell viability. The viability of pCDNA3.1-2- and B1 anti-sense RNA-9-producing GF-1 cells infected with GRNNV were determined at 0, 24, 48, and 72 h post-transfection. Experiments were conducted in triplicate; with each point representing the mean viability from three independent experiments. Error bars represent SEM. Data were analyzed using either paired or unpaired Student's *t*-tests as appropriate. $p<0.05$ was taken to represent a statistically significant difference between mean values of groups.

Annexin V staining revealed enhanced necrosis in antisense B1-overproducing cells (Fig. 6B, panels i–l display phase-contrast micrographs, and panels m–p display red fluorescent micrographs, with annexin V-positive cells indicated by arrows) as compared with the vector control (Fig. 6B, panels a–d display phase-contrast micrographs and panels e–h display red fluorescent micrographs, with annexin V-positive cells indicated by arrows). Furthermore, as shown in Fig. 6C, more necrotic cells (1%, 66%, 81% and 38%) were induced by RGNNV infection in antisense B1–9 cells than in vector (pCDNA3.1)-contained GF-1 cells (1%, 40%, 69% and 99%) at 0, 24 and 48, respectively, but at 72 h p.i., in antisense B1–9 group (38%) was less necrotic cells than vector control group (99%) because in antisense-B1 group, the cells left rarely than vector control group. Moreover, as shown in Fig. 7, the viability of RGNNV-infected, antisense B1–9 cells (100%, 80%, 44%, and 25% at 0, 24, 48, and 72 h p.i., respectively) was lower than that of RGNNV-infected, vector-containing GF-1 cells (100%, 106%, 55% and 38% at the same respective times). In particular, at 24 and 48 h p.i., antisense B1–9-containing cells also displayed reduced cell viability (20% and 10%, respectively) than the vector-containing cells.

Discussion

Early during infection with RGNNV, fish swim abnormally (in circles or to the right) and orient on their sides or belly up (Grotmol et al., 1999; Nakai et al., 1994). Histopathological changes include extensive cellular vacuolation and necrotic neuronal degeneration in

the central nervous system and retina (Grotmol et al., 1999; Nakai et al., 1994). In the present study, we report for the first time that RGNNV B1 is a novel anti-necrotic death mediator during early replication in fish cell systems, which may provide some insights into pathogenesis and disease control.

The RGNNV *B1* gene is expressed from sub-genomic RNA3 in early replication cycle. In previous studies, the sub-genomic RNA RNA3 was predictably synthesized from the 3′ terminus of RNA1 in alphanoviruses and encodes two small proteins designated B1 and B2 (Ball and Johnson, 1999; Schneemann et al., 1998; Johnson et al., 2000). RNA3 was predicted to contain one putative open reading frame encoding the 111 amino acid B1, with the B1-encoding region in the same reading frame as the protein A coding region. Furthermore, synthesis of the nodavirus B1 protein has been confirmed experimentally only for FHV (Harper, 1994). This B1 ORF is the 5′ proximal ORF on FHV RNA3, and only low amounts of this transcript are expressed in FHV-infected *Drosophila* cells.

Based on these findings, Harper (1994) had proposed that low expression may result from a sub-optimal translational initiation context and that the AUG that initiates B1 is only 8 nt from the 5′ end. Furthermore, B1 expression was detected by cDNA clone transfection in NoV-infected insect and animal cells (Johnson et al., 2003), but with betanodavirus infection, only low expression was detected at the cellular level. On the other hand, Iwamoto et al. (2001) reported that RNA3 may lack a *B1* open reading frame entirely. In contrast, from our nucleotide comparison data, the SJNNV strain has a similar open reading frame and a 70% total nucleotide identity with the RGNNV strain (Fig. 1B). These observations are supported by Sommerset and Nerland (2004) and Okinnaka and Nakai (2008), who reported that the RNA1 genome includes the SJNNV RNA3 complete sub-genomic sequence. However, in our system, *B1* is as an early expression gene that was expressed as RNA at 12 h p.i. (Fig. 2A, lane 2) and at the protein level (Fig. 3A, lane 2). Results were consistent in grouper fish cells. Interestingly, according to a study of FHV in the *Drosophila melanogaster* system, B1 expression is very low (Harper, 1994). However, in our system, B1 was highly expressed in three fish cell lines (Fig. 3), such as in grouper liver cells (GL-av), grouper fin cells (GF-1), and zebrafish liver cells (ZLE). With these results above, then we proposed that B1 expression is host cell-dependent, which may provide some important factors for B1 expression during replication that are provided by different cell types (Delsert et al., 1997).

Why does RGNNV encode a novel anti-necrotic protein B1 expressed in the early replication stage? During co-evolution with their hosts, viruses have developed multiple strategies for the manipulation of biological processes in infected cells, including regulation of host cell proliferation, differentiation, and death (Everett and McFadden, 1999). It is well established that many viruses inhibit apoptosis, a strategy that subverts one of the most ancient (non-immune) anti-viral mechanisms, namely the apoptotic suppression of infected cells, and thereby allows the virus to replicate before its host cell dies (Bendict et al., 2002; Gillet and Brun, 1996). Moreover, viruses may also induce apoptosis in either infected cells or in immunologically relevant cells, with the purpose of increasing viral spread or subverting the host's immune response (Bendict et al., 2002; Gillet and Brun, 1996). Mechanisms of betanodavirus enhancement of viral replication strategies are largely unknown.

Does B1 have an anti-death function? B1 protein function remains unknown. Previous alphanodavirus studies using loss-of-function for removing the B1 ORF have suggested that the B1 protein is dispensable for RNA replication in mammalian and yeast cells (Ball, 1995; Eckerle and Ball, 2002; Price et al., 2000). In the present study, we discovered that B1 may have a novel role as an anti-necrotic cell death function (Gillet and Brun, 1996; Boya et al., 2004) which may correlate with maintenance of host mitochondria function (Fig. 5).

The Bcl-2 family of proteins, comprised of both anti- and pro-apoptotic molecules, constitutes a critical, intracellular decision point regulating a common death pathway (Farrow and Brown, 1996). The ratio of antagonist (Bcl-2, Bcl-x_L, Mcl-1, and A1) to agonist (Bax, Bak, Bcl-x_s and Bad) molecules dictates whether a cell responds to a proximal apoptotic stimulus (Farrow and Brown, 1996; Oltvai et al., 1993). These proteins also interact with mitochondria to control the balance of mitochondrial membrane potential (Zamzami and Kroemer, 2001). Apoptosis is controlled at the mitochondrial level by the sequestration of a series of apoptotic proteins including, cytochrome c, Smac/DIABLO, apoptosis inducing factor (AIF), and endonuclease G in the mitochondrial intermembrane space, which facilitates the cytosolic release of these factors upon exposure to proapoptotic signals (Wang, 2001; Ferri and Kroemer, 2001). We have found that B1 is not a Bcl-2 family member due to a lack of similarity to the Bcl-2 family (BH) domain protein sequence (data not shown). So, in this novel viral protein how to regulate the mitochondrial membrane potential remains unknown.

Interestingly, we found that B1 contains nuclear targeting sequences, as shown in Fig. 1, Boxes B1 and B2, between amino acids 33–38 (PRRARAA) and 66–70 (KRPRR). In the NLS study of B1, we have linked the B1 protein to EYFP (Chalfie et al., 1994; Maniak et al., 1995) for direct monitoring its intracellular localization. EYFP-B1-fused proteins were transported into the nucleus (data not shown), but how nuclear B1 protein might regulate mitochondrial events remains unknown. Moreover, knockdown of B1 by its antisense sequence enhances necrotic cell death (Fig. 6) and reduces cell viability (Fig. 7) at the early replication stage, which is consistent with its proposed function.

In summary, in fish cells, we found that B1, a novel protein encoded in viral sub-genomic RNA3, has a low level of expression in the early replication cycle, but shows a large increase in expression after 24 h p.i. Furthermore, in gain-of-function studies, over expression of *B1*) can protect cells against necrotic cell death following RGNNV infection. Finally, in loss-of-function studies, knockdown of B1 expression can enhance cell death. These results in our fish system may provide new insights into RNA viral infection and disease control.

Materials and methods

Cell culture and reagents

The grouper fin cell line (GF-1) was obtained from Dr. Chi (Institute of Zoology and Development of Life Science, Taiwan, ROC) and the zebrafish liver cell line (ZLE) was purchased from the American Type Culture Collection (Manassas, VA). GL-av was subcloned from grouper liver cell line (GL-a), which was obtained from Dr. Yang (Institute of Biotechnology, National Cheng Kung University, Taiwan, ROC). All cell lines were grown at 28 °C in Leibovit's L-15 medium (GibcoBRL, Gaithersburg, MD) supplemented with 5% fetal bovine serum and 25 μg/ml gentamycin. The DIG-RNA labeling kit and annexin V-Alexa 568 staining kit were purchased from Roche Diagnostics (Mannheim, Germany). The nuclear staining dye 4′,6-diamidino-2-phenylindole (DAPI) was purchased from Sigma-Aldrich (St. Louis, MO). The ECL Western blot detection system kit was purchased from Amersham (Piscataway, NJ).

Virus

Naturally infected red grouper larvae collected in 2002 in the Tainan prefecture were the source of redspotted grouper nervous necrosis virus *T*ainan *N*o. *1* (RGNNV TN1), which was used to infect GL-av cells. The virus was purified as previously described (Chen et al., 2006b; Mori et al., 1992) and was stored at −80 °C until use.

Cloning and sequence analysis of RGNNV B1

Synthesis and amplification of cDNAs were performed using the SuperScript™ One-Step reverse transcription-polymerase chain reaction (RT-PCR) kit (Life Technologies, Gibco BRL) according to the manufacturer's instructions. RT-PCR primers NNV B1 P1 (5′-ACCATgTCTgTCgCATTAgA-3′) and NNV B1 P2 (5′-CTCACTTgAgTgC-gACgTC-3′) were used to amplify a fragment covering the variable region of *B1*. Primers P1 and P2 were (final concentration, 0.2 μM) were used in PCR reactions with cycling conditions of 54 °C for 30 min, 2 min at 94 °C, 95 °C for 30 s, 57 °C for 30 s, and 72 °C for 45 s for a total of 35–40 cycles. The purity and size of the amplified product was checked by 1.5% agarose gel electrophoresis after staining with ethidium bromide (Wu et al., 2008). The 336 bp, double-stranded cDNA was purified using the QIAquick™ gel extraction system (Qiagen, Valencia, CA) and subcloned using a pGEMT-easy™ cloning system (Promega, Madison, WI). Cloned PCR products were sequenced by the dye termination method using an ABI PRISM 477 DNA sequencer (PE Biosystems, Foster City, CA) and scanned against the GenBank database BLAST (www4.ncbi.nlm.nih.gov/) and PROSITE (psort.ims.u-tokyo.ac.jp/) programs.

Expression of B1 recombinant protein as an antigen

E. coli BL21(DE3)/pLysS cells were transformed with pET29a, which contains a B1 gene inserted between the EcoRI and Hind III restriction sites. Cultures (50 to 200 ml) were incubated with 0.5 to 2.0 ml of preculture overnight. Optimal expression was obtained by induction with 1 mM IPTG (isopropyl-β-D-thiogalactopyranoside) when cultures reached an optical density of 0.5 at 600 nm (OD_{600}) (Sambrook et al., 1999; Lellouch and Geremia, 1999). Expression of recombinant B1 was monitored by sodium dodecyl sulfate (SDS)-12% polyacrylamide gel electrophoresis (PAGE) (Laemmli, 1970), followed by staining with Coomassie brilliant blue R-250. For identification of the B1 protein using the N-terminus His tag, the gels were subjected to Western blot immunodetection (Kain et al., 1994). Blots were incubated with a 1:15,000 dilution of an anti-His tag polyclonal antibody followed by a 1:7500 dilution of a peroxidase-labeled goat anti-rabbit conjugate (Amersham Biosciences, Piscataway, NJ). Binding was detected by chemiluminescence and captured on Kodak XAR-5 film (Eastman Kodak, Rochester, NY). Recombinant B1 protein was further purified using a Ni^{2+} affinity column (Qiagen). Cell pellets were resuspended in 4 ml of binding buffer (pH 7.8, 20 mM sodium phosphate, 500 mM NaCl) per 100 ml of cell culture, and then lysozyme was added to a final concentration of 1 mg/ml. The cell suspension was incubated on ice for 30 min and then on a rocking platform for 10 min at 4 °C. Triton X-100, DNase, and RNase were added to final concentrations of 1%, 5 μg/ml, and 5 μg/ml, respectively, and samples were incubated for an additional 10 min. The insoluble debris was removed by centrifugation at 3000 g (5000 rpm in a Sorvall SS-34 rotor) for 30 min at 4 °C. The supernatant was loaded on a $Ni2^{+}$ affinity column for binding to resin and the column was flushed with 6 volumes of binding buffer followed by 4 volumes of wash buffer (pH 6.0, 20 mM sodium phosphate, 500 mM NaCl). The bound protein was eluted with 6 volumes of 10, 50, 100 and 150 mM imidazole elution buffer (pH 6.0, 20 mM sodium phosphate, 500 mM NaCl, 10 mM–150 mM imidazole) (Malabika et al., 2007). Column wash fractions were assayed for the presence of the polyhistidine-tagged protein by analyzing 20-μl aliquots by electrophoresis through a 10% SDS-polyacrylamide gel.

Preparation of B1 polyclonal antibody for against RGNNV B1

A New Zealand rabbit was subcutaneously immunized twice every two weeks with 500 μg/1.2 mL of purified recombinant B1 protein emulsified in an equal volume of Freund's complete adjuvant, boosted with 600 μg of antigen emulsified in an incomplete adjuvant at the seventh week. Thirty milliliters was bled from the rabbit during week 8. Collected serum was precipitated with 50% $(NH_4)_2SO_4$, dialyzed against a 0.1 M phosphate buffer pH 8.0 (PB), and purified by protein A chromatography (Pharmacia). The immunoglobulin fraction eluted at pH 3.0 was collected and dialyzed against phosphate buffered saline (PBS). The anti-B1 polyclonal antibodies obtained were aliquoted and frozen at −70 °C and the column was reequilibrated with PB buffer containing 0.05% sodium azide (Hong et al., 1993).

Total mRNA preparation

GF-1 cells were cultured by seeding 10^5 cells/ml in 60 mm diameter petri dishes for 20 h prior to rinsing the monolayers twice with phosphate buffered saline (PBS). Cells were infected with RGNNV-TN 1 at a multiplicity of infection (m.o.i.) of 1 for 0, 12, 24, and 48 h at 28 °C. Total RNA was extracted from mock GF-1-infected control cells and RGNNV-infected GF-1 cells using the TRIzol reagent (Life Technologies) according to the manufacturer's protocol.

Northern blot analysis

Samples containing 1 μg of total RNA of GF-1 and RGNNV-infected GF-1 cells were fractionated on a 1.2% agarose gel containing 5.5% formaldehyde and 1× MOPS, and the separated RNA species were electrically transferred to a nylon membrane (Amersham) as previously described (Sambrook et al., 1999). The transferred RNA was fixed to the membrane by ultraviolet crosslinking. An anti-sense cRNA probe labeled with digoxigenin (DIG) was generated from a digested cDNA insert using a Dig Northern Starter Kit (Roche Diagnostic Corporation, Indianapolis, IN) by in vitro transcription. The membrane was prehybridized and then hybridized according to the manufacturer's protocol. Hybridization was detected using chemiluminescent detection (Holtke et al., 1995).

Western blot analysis

GF-1, GL-av, and ZLE cells cultured as described above were infected with RGNNV TN1 at a m.o.i.=1 and propagation/titration in GF-1 cells with a $TCID_{50}$ of 10^8/0.1 ml) for 0, 12, 24, 48, and 72 h. In the EYFP and EYFP-B1 transfection groups, 3×10^5 GF-1 cells were seeded in 60 mm diameter culture dishes one day before the transfection procedure. The next day, 2 μg of either pEYFP or pEGFP-B1 was added to these cells using Lipofectamine-Plus™ (Life Technologies) prior to incubation for 0, 24, or 48 h. At each time point, the culture medium was aspirated, cells were washed with PBS, and lysed in 0.3 ml of lysis buffer (10 mM Tris, 20% glycerol, 10 mM sodium dodecyl sulfate [SDS], 2% β-mercaptoethanol, pH 6.8). An aliquot of the lysate was used for the separation of proteins by SDS-polyacrylamide gel electrophoresis (Laemmli, 1970). The gels were subjected to immunoblotting (Kain et al., 1994) with 1:3000 dilutions of anti-GRNNV protein A, RGNNV protein α, RGNNV B2, RGNNV B1 polyclonal antibody, or β-actin and EGFP monoclonal antibody, followed by a 1:10,000 dilution of peroxidase-labeled goat anti-rabbit or mouse conjugate antibodies (Amersham Biosciences). Chemiluminescence, indicative of antibody binding, was captured on Kodak XAR-5 film (Eastman Kodak, Rochester, NY).

RGNNV B1-containing stable cell lines

A *B1* coding sequence from RGNNV *B1* (*B1* cDNA in pGEMT-easy plasmid) was amplified using the sense primer 5′-GAAGATCTAC-CATGGTCTGTCGCATT-3′ (BagII recognized site is underlined, the start codon of B2 is in boldface) and an anti-sense primer 5′-CCCAAGCTTC-TACACTTGAGTGCGAC-3′ (HindIII recognized site is underlined). After BagII and HindIII-mediated restriction digestion, the PCR product was ligated with identically an predigested pEYFP-C1 vector (BD

Biosciences ClonTech, Palo Alto, CA) to create pEYFP-B1. Cells producing EYFP or EYFP-B1 were obtained by transfection of GF-1 cells with the pEYFP-C1 or pEYFP-B1 vectors, respectively, and selection with G418 (800 μg/ml). In these vectors, transcription of insert sequences is driven by the immediate-early promoter of human cytomegalovirus. Selection time (2.5–3 months) varied depending on cell-dependent properties (Chen et al., 2006b).

Annexin-V-FLUOS and -Alexa 568 staining

An analysis of phosphatidylserine on the outer leaflet of apoptotic and necrotic cell membranes was performed by using annexin V-fluorescein and propidium iodide (PI) that was used to identify necrotic cells. GF-1-EYFP-3 and GF-1-EYFP-B1–5 cells (10^5/ml) were cultured to monolayer confluence in 60 mm diameter Petri dishes for 20 h and then rinsed twice with PBS. Cells remained uninfected or were infected with RGNNV during incubation at 28 °C for 0, 24, 48, and 72 h. At each time point, the medium was removed from sets of petri dishes, the monolayers were washed with PBS, and the cells were incubated with 100 μl of staining solution (annexin V-fluorescein in a HEPES buffer containing PI; Boehringer-Mannheim, Mannheim, Germany) for 10–15 min. Cells were examined using fluorescence microscopy with 488-nm excitation and a 515-nm long-pass filter for detection annexin V-fluorescein (Chen et al., 2006a) and 515-nm excitation and a 595-nm long-pass filter for detection annexin V-fluorescein.

Evaluation of mitochondrial membrane potential with a lipophilic cationic dye

GF-1-EYFP-3 and GF-1-EYFP-B1–5 cells (10^5/ml) were cultured to monolayer confluence in 60 mm diameter Petri dishes for 20 h and then rinsed twice with PBS. Cells remained uninfected or were infected with RGNNV during incubation at 28 °C for 0, 24, 48, and 72 h. At each time point, the medium was removed from sets of petri dishes, the monolayers were washed with PBS, 500 μl of diluted MitoCapture reagent (Mitochondria BioAssay™ Kit; BioVision, Mountain View, CA) was added, and each dish was incubated at 37 °C for 15–20 min (Chen et al., 2006a). The cells were examined immediately under a fluorescence microscope using 488 nm excitation and a 515 nm long-pass filter for detection of fluorescein and 510 nm excitation and a 590 nm long-pass filter for detection of rhodamine.

Quantification of cell viability

Approximately 10^5 cells/ml expressing GF-1-EYFP-3 or GF-1-EYFP-B1–5 were cultured in a 60 mm diameter Petri dish for 20 h. RGNNV-infected EYFP- and EYFP-B1 expressing GF-1 cells (m.o.i.=1) and uninfected cells were then incubated at 28 °C for 0, 24, 48, or 72 h. At each time point, sets of petri dishes were washed with PBS and treated with 0.5 ml of 0.1% trypsin-EDTA (Gibco, Grand Island, NY) for 1–2 min. Cell viability was determined in triplicate using a Trypan blue dye exclusion assay (Mullen et al., 1975). Each data point represents the mean viability of three independent experiments±SEM. Data were analyzed using either paired or unpaired Student's *t*-tests as appropriate. A value of $p<0.05$ was taken to represent a statistically significant difference between mean values of groups.

Selection of RGNNV B1-anti-sense RNA-containing stable cell lines

A *B1* anti-sense sequence from RGNNV *B1* (*B1* cDNA in pGEMT-easy plasmid) was amplified using the anti-sense primer (p1) 5′-ACCATGTCTGTCGCATTAGA-3′ and the sense primer (p2) 5′-CTA-CACTTGAGTGCGACGTC-3′. The PCR product was ligated with pCDNA3.1/V5-His TOPO vector (Promega, Madison, WI) to create pCDNA3.1/V5-His TOPO-RGNNV-antisense B1. Vector- (TOPO; as a negative control) and RGNNV-antisense B1-producing cells were obtained by transfection of GF-1 cells with the pCDNA3.1/V5-His TOPO and pCDNA3.1/V5-His TOPO-RGNNV-antisense B1 vectors, respectively and selection with G418 (800 μg/ml). In these vectors, transcription of insert sequences is driven by the immediate-early promoter of human cytomegalovirus. Selection time (2.5–3 months) varied depending on cell-dependent properties (Chen et al., 2006b).

Cell counts

Virus-infected GF-1-EYFP-3 and GF-1-EYFP-B1–5 cells were labeled with annexin V-fluorescein. The number of positive cells in 200 cells per sample was assessed in three individual experiments. Results are expressed as the mean±standard error of the mean (SEM). Data were analyzed using either paired or unpaired Student's *t*-tests, as appropriate. A value of $p<0.05$ was taken to represent a statistically significant difference between group mean values.

Acknowledgments

The authors are grateful to Dr. H. L. Yang (Institute of Biotechnology, National Cheng Kung University, Taiwan, ROC) for providing the grouper liver cell line GL-a, to Dr. S. C. Chi (Institute of Zoology and Development of Life Science, Taiwan, ROC) for providing the grouper fin cell line GF-1, and to Dr. J. L. Wu (Institute of Cellular and Organismic Biology, Academia Sinica, Nankang, Taipei 115, Taiwan, Taiwan, ROC) for comments on the manuscript. This work was supported by grants (NSC-94-2313-B-006-002; NSC-95-2313-B-006-003) awarded to Dr. Jiann-Ruey Hong from the National Science Council, Taiwan, ROC.

References

Ball, L.A., 1995. Requirements for the self-directed replication of flock house virus RNA1. J. Virol. 69, 720–727.
Ball, L.A., Johnson, K.L., 1999. Reverse genetics of nodaviruses. Advances in Virus Res. 53, 229–244.
Bendict, C.A., Norris, P.S., Ware, C.F., 2002. To kill or be killed: viral evasion of apoptosis. Nat. Immunol. 3, 1013–1018.
Bovo, G., Nishizawa, T., Maltese, C., Borghesan, F., Mutinelli, F., Montesi, F., DeMass, S., 1999. Viral encephalopathy and retinopathy of farmed marine fish species in Italy. Virus Res. 63, 143–146.
Boya, P., Pauleau, A.L., Poncet, D., Gonzalez-Polo, R.A., Zamzami, N., Kroemer, G., 2004. Viral proteins targeting mitochondria: controlling cell death. Biochimica. et Biophysica. Acta. 1659, 178–189.
Chalfie, M., Tu, Y., Euskirchen, G., Ward, W.W., Prasher, D.C., 1994. Green fluorescent protein as a marker for gene expression. Science 263, 802–805.
Chen, S.P., Yang, H.L., Her, G.M., Lin, H.Y., Jeng, M.F., Wu, J.L., Hong, J.R., 2006a. NNV induces phosphatidylserine exposure and loss of mitochondrial membrane potential in secondary necrotic cells, both of which are blocked by bongkrekic acid. Virology 347, 379–391.
Chen, S.P., Yang, H.L., Her, G.M., Lin, H.Y., Chen, M.C., Wu, J.L., Hong, J.R., 2006b. Enhanced viability of a nervous necrosis virus infected stable cell line over-expressing a fusion product of the zfBcl-x_L and green fluorescent protein genes. J. Fish Dis. 29, 347–354.
Chen, S.P., Wu, J.L., Su, Y.C., Hong, J.R., 2007. Anti-Bcl-2 family members, zfBcl-x_L and zfMcl-1a, prevent cytochrome *c* release from cells undergoing betanodavirus-induced secondary necrotic cell death. Apoptosis 12, 1043–1060.
Criddle, D.N., Gerasimenko, J.V., Baumgartner, H.K., Jaffar, M., Voronina, S., Sutton, R., Petersen, O.H., Gerasimenko, O.V., 2007. Calcium signaling and pancreatic cell death: apoptosis or necrosis? Cell Death Differ. 14, 1285–1294.
Delsert, C., Morin, N., Comps, M., 1997. Fish nodavirus lytic cycle and semipermissive expression in mammalian and fish cell cultures. J. Virol. 71, 5673–5677.
Eckerle, L.D., Ball, L.A., 2002. Replication of the RNA segments of a bipartite viral genome is coordinated by a transactivating sub-genomic RNA. Virology 296, 165–176.
Everett, H., McFadden, G., 1999. Apoptosis: an innate immune response to virus infection. Trends Microbiol. 7, 1600–3165.
Falquet, L., Pagni, M., Bucher, P., Hulo, N., Sigrist, C.J., Hofmann, K., Bairoch, A., 2002. The PROSITE database, its status in 2002. Nucleic Acids Res. 30, 235–238.
Farrow, S.N., Brown, R., 1996. New members of the Bcl-2 family and their protein partners. Cur. Opin. Gene. Dev. 6, 45–49.
Ferri, K.F., Kroemer, G., 2001. Organelle-specific initiation of cell death pathways. Nat. Cell Biol. 3, E255–E263.
Gillet, G., Brun, G., 1996. Viral inhibition of apoptosis. Trends Microbio. 4, 312–316.
Grotmol, S., Beerfh, O., Totland, G.K., 1999. Transmission of viral encephalopathy and retinopathy (VER) to yolk-sac larvae of the Atlantic halibut hippoglossus:

occurrence of nodavirus in various organs and a possible route of infection. Dis. Aquat. Organ. 36, 95–106.
Gukovskaya, A.S., Vaquero, E., Zaninovic, V., Gorelick, F.S., Lusis, A.J., Brennan, M.L., et al., 2002. Neutrophils and NADPH oxidase mediate intrapancreatic trypsin activation in murine experimental acute pancreatitis. Gastroenterology 122, 974–984.
Guo, Y.X., Wei, T., Dallmann, K., Kwang, J., 2003. Induction of caspase-dependent apoptosis by betanodaviruses GGNNV and demonstration of protein α as an apoptosis inducer. Virology 308, 74–82.
Harper, T.A., 1994. Characterization of the proteins encoded from the nodaviral subgenomic RNA. Ph.D. Thesis. University of Wisconsin-Madison.
Hong, J.C., Hong, T.H., Chang, J.G., Chang, T.H., 1993. Production and characterization of monoclonal antibodies against αand β spectrin subunits. J. Formos. Med. Assoc. 92, 61–67.
Holtke, H.J., Ankenbauer, W., Muhleggerk, K., Rein, R., Sanger, G., Seibl, R., Walter, T., 1995. The digoxigenin (DIG) system for non-radioactive labeling and detection of nucleic acids—an overview. Cell Mol. Biol. 41, 883–905.
Iwamoto, T., Mise, K., Mori, K., Arimoto, M., Nakai, T., Okuno, T., 2001. Establishment of an infectious RNA transcription system for *striped jack nervous virus*, the type species of the betanodaviruses. J. Gen. Virol. 82, 2653–2662.
Iwamoto, T., Mise, K., Takeda, A., Okinaka, Y., Mori, K., Arimoto, M., Okuno, T., Nakai, T., 2005. Characterization of striped jack nervous necrosis virus subgenomic RNA3 and biological activities of its encoded protein B2. J. Gen. Virol. 86, 2807–2816.
Johnson, K.L., Zeddam, L.L., Ball, L.A., 2000. Characterization and construction of functional cDNA clones of pariacoto virus, the first alphanodavirus isolated Australasia. J. Virol. 74, 5123–5132.
Johnson, K.L., Price, B.D., Ball, A., 2003. Recovery of infectivity from cDNA clones of nodamura virus and identification of small nonstructural proteins. Virology 305, 436–451.
Kain, S.R., Mai, K., Sinai, P., 1994. Human multiple tissue Western blots: a new immunological tool for the analysis of tissue-specific protein expression. BioTechniques 17, 982–987.
Kerr, J.F.R., Harmon, B.V., 1991. Definition and incidence of apoptosis: an historical perspective. In: Tomei, L.D., Cope, F.O. (Eds.), Apoptosis: The Molecular Basis of Cell Death. Cold Spring Harbor Laboratory Press, Cold Spring Harbor, pp. 5–29.
Laemmli, U.K., 1970. Cleavage of structural proteins during the assembly of the head of bacteriophage T4. Nature 227, 680–685.
Lellouch, A.C., Geremia, R.A., 1999. Expression and study of recombinant ExoM, a β1–4 glucosyltransferase involved in succinoglycan biosynthesis in sinorhizobium meliloti. J. Bacteriol. 181, 1141–1148.
Li, H., Li, W.X., Ding, S.W., 2002. Induction and suppression of RNA silencing by an animal virus. Science 296, 1319–1321.
Lu, R., Maduro, M., Li, F., Li, H.W., Broitman-Maduro, G., Li, W.X., Ding, S.W., 2005. Animal virus replication and RNAi-mediated antiviral silencing in *Caenorhabditis elegans*. Nature 436, 1040–1043.
Majno, G., Joris, I., 1995. Apoptosis, oncosis and necrosis: an overview of cell death. Am. J. Pathol. 146, 3–15.
Malabika, D., Ganguly, T., Chattoraj, P., Chanda, P.K., Bandhu, A., Lee, C.Y., Sau, S., 2007. Purification and characterization of repressor of temperate S. aureus phage phi11. J. Bichem. Mol. Biol. 40, 740–748.
Maniak, M., Rauchenberger, R., Albrecht, R., Murphy, J., Gerisch, G., 1995. Coronin involved in phagocytosis: dynamics of particle-induced relocalization visualized by a green fluorescent protein tag. Cell 83, 915–924.
Michaud, S., Lavoie, S., Guimond, M.O., Tanguay, R.M., 2008. The nuclear localization of *Drosophila* Hsp27 is dependent on a monopartite arginine-rich NLS and is uncoupled from its association to nuclear speckles. Biochimica Biophysica Acta 1783, 1200–1210.
Mori, K., Nakai, T., Muroga, K., Arimoto, M., Mushiake, K., Furusawa, I., 1992. Properties of a new virus belongs to *Nodaviridae* found in larval striped jack (*Pseudocaranx dentex*) with nervous necrosis. Virology 187, 368–371.
Mullen, P.D., Brand, R.J., Parlette, G.N., 1975. Evaluation of dye exclusion and colony inhibition techniques for detection of polyoma-specific, cell-mediated immunity. J. Natl. Cancer Inst. 54, 229–231.
Munday, B.L., Kwang, J., Moody, N., 2002. Betanodavirus infections of teleost fish: a review. J Fish Dis. 25, 127–142.
Nakai, T., Nguyen, H.D., Nishizawa, T., Muroga, K., Arimoto, M., Octsuki, K., 1994. Occurrence of viral nervous necrosis in kelp grouper and tiger puffer. Fish Pathol. 29, 211–212.
Nagai, T., Nishizawa, T., 1999. Sequence of the non-structural protein gene encoded by RNA1 of atriped jack nervous necrosis virus. J. Gen. Virol. 80, 3019–3022.
Nishizawa, T., Mori, K., Furuhashi, M., Nakai, T., Furusawa, I., Muroga, K., 1995. Comparison of the coat protein genes of five fish nodaviruses, the causative agents of viral nervous necrosis in marine fish. J. Gen. Virol. 76, 1563–1569.
Ng, A.K., Zhang, H., Tan, K., Li, Z., Liu, J.H., Chan, P.K., Li, S.M., Chan, W.Y., Au, S.W., Joachimiak, A., Waiz, T., Wang, J.H., Shaw, P.C., 2008. Structure of influenza virus A H5N1 nucleoprotein: implications for RNA binding, oligomerization, and vaccine design. FASEB J. 22 (10), 3638–3647.
Okinnaka, Y., Nakai, T., 2008. Comparisons among the complete genomes of four betanodavirus genotypes. Dis Aquat Organ. 80 (2), 113–121.
Oltvai, Z.N., Milliman, C.L., Korsmeyer, S.J., 1993. Bcl-2 hetrodimerizes in vivo with a conserved homolog, Bax, that accelerates programmed cell death. Cell 74, 609–619.
Price, B.D., Roeder, M., Ahlquist, P., 2000. DNA-directed expression of function flock house virus RNA1 derivatives in *Saccharomyces cerevisiae*, heterologous gene expression, and selective effects on subgenomic mRNA synthesis. J. Virol. 74, 11724–11733.
Sambrook, J., Fritsch, E.M., Maniatis, T., 1999. Molecular Cloning: A Laboratory Manual, 2nd Edition. Cold Spring Harbor Laboratory, Cold Spring Harbor Labor, New York.
Schneemann, A., Reddy, V., Johson, J.E., 1998. The structural and function of nodavirus particles: a paradigm for understanding chemical biology. Advances in Virus Res. 50, 381–446.
Schwab, B.L., Guerini, D., Didszun, C., Bano, D., Ferrando-May, E., Fava, E., Tam, J., Xu, D., Xanthoudakis, S., Nicholson, D.W., Carafoli, E., Nicotera, P., 2002. Cleavage of plasma membrane calcium pumps by caspases: a link between apoptosis and necrosis. Cell Death Differ 9, 818–831.
Sommerset, I., Nerland, A.H., 2004. Complete sequence of RNA1 and subgenomic RNA3 of Atlantic halibut nodavirus (AHNV). Dis. Aquat. Org. 58, 117–125.
Su, Y.C., Wu, J.L., Hong, J.R., 2009. Betanodavirus non-structural protein B2: A novel necrotic death factor that induces mitochondria-mediated cell death in fish cells. Virology 385, 143–154.
Toffolo, V., Negrisolo, E., Maltese, C., Bovo, G., Belvedere, P., Colombo, L., Valle, L.D., 2006. Phylogeny of betanodaviruses and molecular evolution of their RNA polymerase and coat proteins. Mol. Phylogenet. Evol. 43 (1), 298–308.
Wang, X., 2001. The expanding role of mitochondria in apoptosis. Genes Dev. 15, 2922–2933.
Wang, X.H., Aliyari, R., Li, W.X., Li, H.W., Kim, K., Carthew, R., Atkinson, P., Ding, S.W., 2006. RNA interference directs innate immunity against viruses in adult *Drosophila*. Science 312, 452–454.
Weiss, B., Davidkova, G., Zhou, L.W., 1999. Antisense RNA gene therapy for studying and modulating biological processes. CMLS Cell. Mol. Life Sci. 55, 334–358.
Wu, H.C., Chiu, C.S., Wu, J.L., Gong, H.Y., Chen, M.C., Lu, M.W., Hong, J.R., 2008. Zebrafish anti-apoptotic protein zfBcl-x(L) can block betanodavirus protein alpha-induced mitochondria-mediated secondary necrosis cell death. Fish Shellfish Immunol. 24, 436–449.
Wyllie, A.H., Kerr, J.F.R., Currie, A.R., 1980. Cell death: the significance of apoptosis. Int. Rev. Cytol. 68, 251–306.
Zamzami, N., Kroemer, G., 2001. The mitochondrion in apoptosis: how Pandora's box opens. Nat. Rev. Mol. Cell Biol. 2, 67–71.